

**Gently lifting gold's herringbone reconstruction: Trimethylphosphine on Au(111)**

April D. Jewell, Heather L. Tierney, and E. Charles H. Sykes\*

*Department of Chemistry, Tufts University, Medford, Massachusetts 02155-5813, USA*

(Received 3 September 2010; revised manuscript received 4 October 2010; published 3 November 2010)

Alkane thiol self-assembled monolayers form the backbone of many surface technologies but the true complexity of these molecule-metal interfaces has only recently been realized. Here we report a phosphine-based system that self-assembles with surface restructuring that is markedly different than that observed with thiols. Our results reveal the atomic-scale mechanism by which trimethylphosphine removes gold's native reconstruction but, unlike thiols, stops short of removing further surface atoms. Our results also suggest that self-assembly may be controlled and improved by adjusting the molecule-metal bond strength.

DOI: [10.1103/PhysRevB.82.205401](https://doi.org/10.1103/PhysRevB.82.205401)

PACS number(s): 68.43.Hn, 68.37.Ef

**I. INTRODUCTION**

Self-assembled monolayers (SAMs) are considered a robust tool in many areas of nanotechnology and have multiple uses in sensing, lubrication, corrosion inhibition, patterning, and device self-assembly. The most common types of SAMs are derived from alkane thiols adsorbed on metal surfaces, typically Au in order to take advantage of the strong Au-S bond. Very recently researchers discovered that the structure of the molecule-metal interface in thiol-based SAMs is much more complex than first believed.<sup>1-5</sup> Clean Au exhibits the unique  $22 \times \sqrt{3}$  unit cell, or “herringbone” reconstruction, which arises due to the compression of atoms in the topmost layer of the crystal. The compression results in an extra 4.4% Au atoms in the surface layer and gives rise to a periodic array of fcc-stacked and hcp-stacked regions separated by soliton walls (where the surface-most atoms traverse bridge sites). A pair of soliton walls are collectively termed the herringbone. Many species, including thiols, have recently been shown to lift the herringbone reconstruction of Au(111) (i.e., remove the extra 4.4% Au atoms), resulting in a  $(1 \times 1)$  surface structure.<sup>1-8</sup> Thiols further remove a significant portion of the remaining Au surface atoms,<sup>1,3,5,9-13</sup> and the etch pits formed by the vacancies are known to be one of the weakest areas of the SAM films in terms of attack and degradation by oxidizing species.<sup>14</sup> The mechanism by which thiols lift Au's herringbone is still under debate; however, Yates and co-workers have shown that dimethyl dithiol SAMs evolve via a well-defined “stripe phase” in which the liberated Au adatoms are each attached to two thiolate species.<sup>1,9,11</sup> The number of Au atoms in the stripe phase can be directly correlated with the number of atoms removed from the herringbone reconstruction.<sup>1</sup> Given this bonding scheme, with a 2:1 thiolate to Au adatom ratio, the formation of etch pits is expected as alkane thiol coverage increases to  $>0.1$  ML, or more specifically, when the excess 4.4% atoms in the herringbone have been depleted. Understanding the atomic-scale surface processes that occur when molecules bind to Au(111) is a crucial step toward improving current films and discovering better and more defect-free routes to the self-assembly of a variety of molecules.<sup>15</sup>

In an effort to weaken the molecule-metal interaction strength and prevent the formation of etch pits, we have chosen to study the interaction and assembly of trimethylphosphine (TMP) on Au(111) using scanning tunneling microscopy (STM). Early macroscopic investigations of trialkylphosphines ( $\text{PR}_3$ ) indicate that they form strongly bound layers on Au(111),<sup>16-20</sup> and that the bond enthalpy of the  $\text{PR}_3$  layer on Au is  $\sim 120$  kJ/mol, which is slightly weaker than that of an adsorbed thiol layer (130–170 kJ/mol).<sup>17,21</sup> The  $\text{PR}_3$  molecules bind via the lone electron pairs on the phosphorous atoms and their alkyl tails point away from the surface.<sup>17</sup>  $\text{PR}_3$  species are widely used in organic synthesis (for C-C bond formation)<sup>22</sup> and as surfactants in the formation of metal nanoparticles,<sup>23</sup> so understanding their interaction with metal substrates on the atomic scale is critical to improving such processes.

By performing experiments in ultrahigh vacuum (UHV) we have been able to study coverage-dependant behavior and the effect of temperature in a controlled manner. Our results indicate that TMP molecules bind strongly to the surface, dramatically changing the surface reconstruction and creating kinetically trapped Au nanoislands. We propose a mechanism by which the Au surface is reorganized, and have found that the degree of surface reorganization can be controlled as a function of coverage and temperature. These films form well-ordered monolayers which are stable at room temperature and desorb molecularly at  $T > 500$  K. Importantly from a self-assembly point of view, no etch pits are formed when TMP adsorbs on Au(111), even at full monolayer coverage.

By performing experiments in ultrahigh vacuum (UHV) we have been able to study coverage-dependant behavior and the effect of temperature in a controlled manner. Our results indicate that TMP molecules bind strongly to the surface, dramatically changing the surface reconstruction and creating kinetically trapped Au nanoislands. We propose a mechanism by which the Au surface is reorganized, and have found that the degree of surface reorganization can be controlled as a function of coverage and temperature. These films form well-ordered monolayers which are stable at room temperature and desorb molecularly at  $T > 500$  K. Importantly from a self-assembly point of view, no etch pits are formed when TMP adsorbs on Au(111), even at full monolayer coverage.

**II. EXPERIMENTAL METHODS**

All STM experiments were performed in a low-temperature, UHV microscope built by Omicron Nanotechnology. The Au(111) sample purchased from MaTeck was prepared under vacuum by cycles of  $\text{Ar}^+$  sputtering (1.5 keV/10  $\mu\text{A}$ ) for 30 min followed by a 2 min anneal to 1000 K. This cycle was repeated approximately 12 times upon receiving the crystal. Between each STM experiment the crystal was prepared by 2 sputter/anneal cycles. After the final anneal, the crystal was transferred in less than 5 min to vacuum ( $<5 \times 10^{-11}$  mbar) to the precooled STM stage. The sample cooled from room temperature to 78 K in approximately 30 min. All images were recorded with cut Pt/Ir tips, and voltages reported refer to the sample bias. Trimethylphosphine, 99% purity, was purchased from Sigma Aldrich and used without further purification. TMP was deposited on

the sample by a collimated molecular doser while the tip was scanning and was always dosed with the metal sample at 78 K and subsequently annealed as noted. The TMP-Au systems could not be stably imaged as dosed at 78 K, and annealing the sample yielded more static systems. This observation indicates a mobile precursor state, such as that observed for benzene on Si,<sup>24</sup> and suggests that the system requires extra energy (i.e., heat) in order for the molecules to equilibrate to their preferred adsorbed state. Molecular coverage values were calculated from molecularly resolved STM images and 1 ML refers to the TMP coverage of a full close-packed ( $\sqrt{7} \times \sqrt{7}$ )R19° layer. Finally, island coverage measurements are reported for images in which both islands and herringbones are present, surveying  $>17\,000\text{ nm}^2$  in each such system. For systems in which no herringbones remain, island coverage measurements were made using several images surveying  $>47\,000\text{ nm}^2$  for each data point.

### III. RESULTS AND DISCUSSION

#### A. Lifting the herringbone and the formation of Au nanoislands

Figure 1(a) shows an STM image of 0.62 ML TMP on Au(111) that has been annealed to 220 K. At this coverage the molecular density was  $1.2 \pm 0.1$  molecules/ $\text{nm}^2$  and the characteristic herringbones of the Au(111) surface were not visible. This observation suggests that the adsorbed molecular layer relieved the inherent strain of the native surface<sup>7</sup> ejecting Au atoms from the herringbone and leading to a  $(1 \times 1)$  surface configuration. The ejected adatoms formed islands, which were themselves covered with molecules and comprised  $0.9 \pm 0.4\%$  of the surface. Line scans over islands, such as those shown in Fig. 1(b), yielded a measured height of  $0.25 \pm 0.05\text{ nm}$ , which is comparable to the height of a monatomic Au step of 0.24 nm. These two observations, coupled with the notable lack of etch pit formation, affirms that the islands were comprised of Au adatoms, which came directly from the extra atoms released from herringbone reconstruction.

In this first experiment, the disappearance of the herringbone reconstruction was concerted with the appearance of Au islands. In order to investigate in detail how the reconstruction lifted, we imaged molecular coverages and annealing temperatures that yielded some Au islands but retained a portion of the herringbone surface reconstruction. This set of experiments allowed us to elucidate the mechanism by which TMP lifted Au's reconstruction by spatially correlating the position of the Au island arrays with that of the Au herringbones. Figures 2 and 3 show STM images of 1.0 ML TMP on a Au(111) surface, after annealing to 220 K. The surface topographies of bare Au and the 1.0 ML TMP systems are compared in Fig. 2. The plots indicate that the Au surface topography (i.e., the height of the soliton walls) is not affected by the TMP molecules, however, it is more difficult to resolve due to the corrugation of the adsorbed molecular layer. At full coverage TMP formed a nearly perfect overlayer, which exhibited hexagonal packing with a close-packed distance of  $0.76 \pm 0.06\text{ nm}$  and a density of  $2.0 \pm 0.1$  molecules/ $\text{nm}^2$ . The unit cell was calculated to be

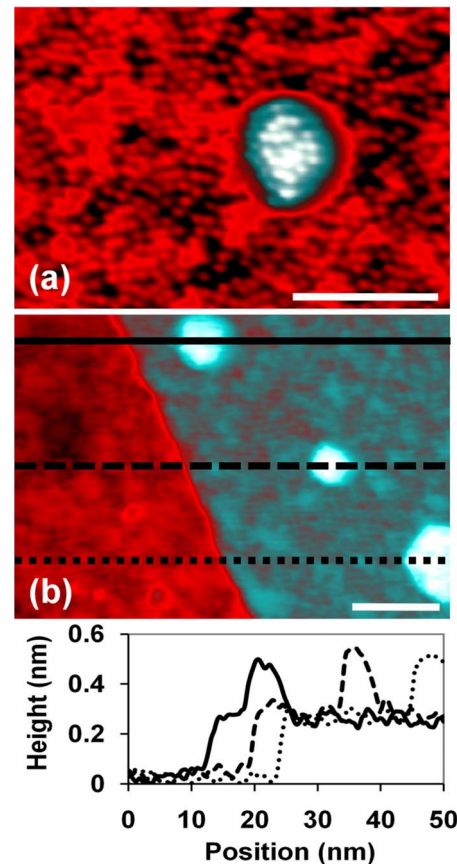


FIG. 1. (Color online) STM images showing 0.62 ML TMP on Au(111); the system has been annealed to 220 K. Line scans, each traversing a single island and a monatomic step edge, indicate that the islands are one gold atom high. Scale bars=10 nm. Imaging conditions: 78 K, (a) 500 pA, 500 mV and (b) 300 pA, 200 mV.

( $\sqrt{7} \times \sqrt{7}$ )R19° using molecular row spacing and angle measurements taken from high-resolution images such as those in Fig. 3. The unit-cell dimensions were confirmed with two-dimensional (2D) Fourier transform analysis. Several small islands were present, covering  $2.4 \pm 0.7\%$  of the surface, and were relatively monodisperse in size:  $5 \pm 2\text{ nm}^2$ . The herringbones were still visible but with an increased unit-cell dimension of  $11.2 \pm 0.9\text{ nm}$ . Finally, there was no evidence for further disruption of the Au surface in the form of vacancies left by ejected atoms (etch pits) in this system. The dark areas in the images shown are vacancies in the adsorbed molecular layer rather than the underlying surface.

Images like those shown in Fig. 3 revealed that at full monolayer coverage the herringbones were fewer in number than on clean Au and that the ejected atoms formed rows of islands parallel to the reconstruction itself. Close inspection of these images suggested that the lifting mechanism involved atoms being ejected from the hcp regions between soliton walls to leave rows of Au atoms in the form of small islands. The middle right side of Fig. 3(a) shows a soliton wall loop that terminates with an ejected Au atom island. This loop marks an area where there is an edge dislocation in the underlying Au surface arising from a mismatch in the atomic rows between the fcc-stacked and hcp-stacked regions.<sup>25</sup> The undercoordination of Au atoms at edge dislo-

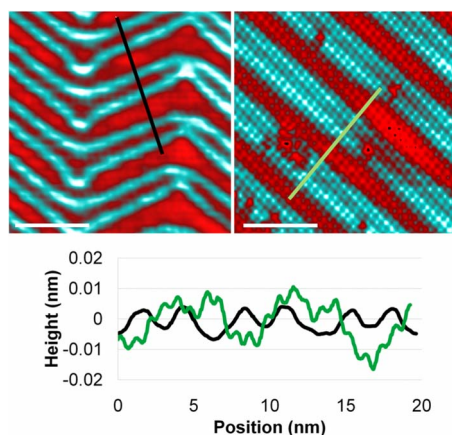


FIG. 2. (Color online) Images of clean Au (top left) and 1.0 ML trimethylphosphine on Au annealed to 220 K (top right), and accompanying line scans (bottom). The plot shows line scans taken over the indicated portion indicated on both the unmodified (black) and modified (green/gray) surfaces. Both plots show the corrugation of Au's herringbone reconstruction in which the soliton walls are slightly higher than the rest of the surface. The plot from the modified surface also shows the corrugation due to the molecular layer which dominates the  $z$  scale making the topographic height modulation due to the soliton walls harder to see in the line scan. Scale bars=10 nm. Image conditions: 78 K, (left) 2 nA, 50 mV and (right) 300 pA, 200 mV.

fications leads to a perturbed electron density which allows these areas to act as preferential binding sites for adatoms and other adsorbates.<sup>26–28</sup> Edge dislocations can also behave as ideal sites though which adatoms can enter and exit the surface layer.<sup>29</sup> As the herringbone was lifted upon TMP adsorption, it is likely that the atoms were ejected at edge dislocations sites like the one shown in Fig. 3(a). Figures 3(b) and 3(c) show a similar arrangement in which edge dislocations have retreated, leaving behind rows of Au islands on top of fcc-packed Au. From an energetic standpoint, these atoms would have ideally migrated to a nearby step edge<sup>30</sup> but they were trapped by the dense TMP layer, had a limited diffusion length, and coalesced into small islands ( $5 \pm 2$  nm<sup>2</sup>). The fact that the Au adatoms formed rows of small islands that closely followed the herringbone strongly suggests that they are kinetically trapped by the surrounding

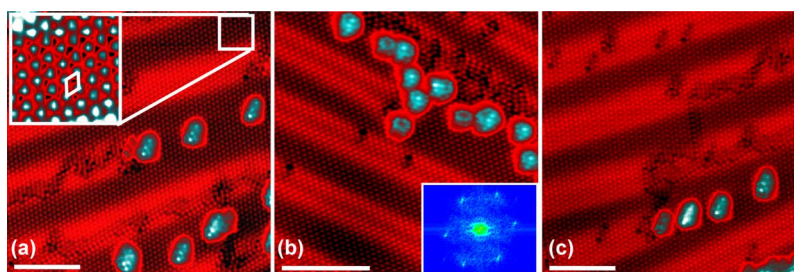


FIG. 3. (Color online) Several STM images showing 1.0 ML TMP on Au(111); the system has been annealed to 220 K. The molecules form a dense, hexagonally packed layer with a  $(\sqrt{7} \times \sqrt{7})R \pm 19^\circ$  unit cell, as shown in the high-resolution inset in (a). 2D Fourier transform analysis—image inset in (b)—supports this unit-cell assignment. These large-scale images reveal that the unit cell of the herringbone reconstruction is larger than on clean Au(111) and that Au islands appear at the positions once occupied by hcp domains. Scale bars = 10 nm. Imaging conditions: 78 K, 300 pA and 200 mV.

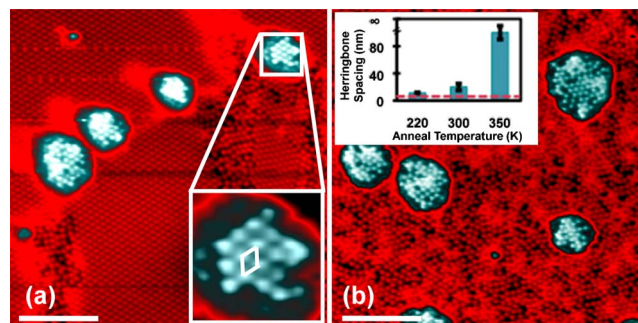


FIG. 4. (Color online) STM images showing TMP on Au(111). The initial coverage system (Fig. 3) was annealed to (a) 300 K and (b) 350 K, resulting in 0.90 ML and 0.88 ML coverages, respectively. In the systems, the Au adatoms originating from the herringbone have a longer diffusion path and coalesce to form large islands. The plot inset in (b) shows the evolution of the herringbone spacing as a function of anneal temperature; the dashed line indicates Au's native herringbone spacing of 6.34 nm. Scale bars = 10 nm. Imaging conditions: 78 K, (a) 300 pA and 200 mV and (b) 200 pA and 200 mV.

TMP layer, similar to the NO<sub>2</sub>/Au(111) system examined by King and co-workers.<sup>8</sup>

The full coverage system shown in Fig. 3 was exposed to a series of controlled annealing treatments, which allowed us to examine the effects of coverage and temperature on the evolution of the TMP-Au system. Figure 4 shows STM images of TMP on Au(111) annealed to (a) 300 K and (b) 350 K; these annealing treatments resulted in systems with similar molecular coverage but with very different molecular packing structures. In the 300 K annealed system, some molecules desorbed, which resulted in an increase in the number of vacancies in the molecular layer. The molecular density dropped slightly to  $1.8 \pm 0.2$  molecules/nm<sup>2</sup> and the herringbone spacing increased to  $20 \pm 5$  nm. The molecule's preference for the fcc region is evident in images like the one shown in Fig. 4(a), where the density of molecules is much higher in the fcc than in the hcp region ( $2.0 \pm 0.1$  versus  $1.6 \pm 0.1$  molecules/nm<sup>2</sup>). Molecules in the densely packed fcc regions maintained the  $(\sqrt{7} \times \sqrt{7})R \pm 19^\circ$  unit cell. The Au islands were larger and with a wider size distribution ( $7 \pm 6$  nm<sup>2</sup>) unlike in the previous system, and covered  $2.1 \pm 0.9\%$  of the surface. When the same system was further

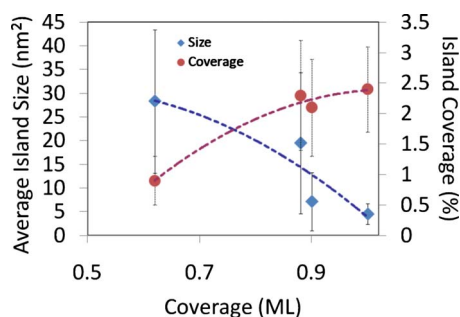


FIG. 5. (Color online) Plot showing percent Au island coverage (red circles) and average island size (blue diamonds) as a function of molecular coverage. As molecular coverage increases, the island coverage increases but the island size decreases. These data indicate that island growth is a kinetically limited process dictated by molecular coverage.

annealed to 350 K, more molecules desorbed and the herringbones were no longer visible, suggesting that the substrate surface had globally adopted a  $(1 \times 1)$  arrangement. The molecular density of this system was  $1.8 \pm 0.1$  molecules/nm<sup>2</sup>; however, regions of densely packed molecules were no longer observed. Au islands covered  $2 \pm 1\%$  of the surface and their placement no longer followed the herringbone reconstruction and appeared to be random. Furthermore, the average island size increased dramatically to  $20 \pm 10$  nm<sup>2</sup>. These observations suggest that island formation and growth is a kinetically limited process at high molecular density. The lower molecular density of the annealed systems allowed the ejected Au adatoms to migrate farther and coalesce to form larger islands as the Au surface globally adopted a  $(1 \times 1)$  fcc configuration.

The herringbone spacing of the high-coverage system evolved as a function of annealing temperature, as shown in Fig. 4(c). The full coverage system, which resulted from dosing molecules at 78 K and then annealing to 220 K, exhibited a herringbone spacing of  $11 \pm 1$  nm, almost twice that of native Au (6.34 nm). Upon annealing this system to 300 K, the herringbone was lifted even further ( $20 \pm 4$  nm), and the herringbones fully disappeared after the 350 K anneal. These data support our hypothesis that the restructuring of Au surface is a kinetically limited process that requires vacant surface sites to induce Au atom ejection. These sites become available as a result of molecular desorption upon annealing the system. A similar lifting of the herringbone reconstruction has been reported for the comparatively large aromatic thiol species Azure A (3-amino-7-(dimethylamino)phenothiazine-5-IUm chloride) adsorbed on Au(111).<sup>31</sup> Azure A adsorption resulted in a maximum increase of 22% in the herringbone spacing (up to 7.7 nm), indicating that it has a weaker interaction with Au than TMP.

Figure 5 illustrates the relationship between molecular coverage and Au island coverage (red circles), as well as average Au island size (blue diamonds). As the molecular coverage increased, the total island coverage increased while the average island size decreased. These observations provide further evidence that the processes under investigation are kinetically limited. At high molecular coverage, ejected Au atoms were trapped among densely packed molecules

and unable to form large islands because island growth was hindered by the short diffusion lengths afforded by the dense molecular layer. This phenomenon can be clearly seen in the evolution of island growth resulting from annealing the full coverage (1.0 ML) system to 300 and 350 K. As stated previously, annealing the system caused molecules to desorb leading to lower coverage systems (0.90 ML and 0.88 ML, respectively). In these systems, Au adatoms diffused rapidly and coalesced into nearby islands, defects, and step edges. The process of molecular desorption led to vacancies in the molecular layer. This process opened surface sites allowing even more atoms to be ejected, and eventually fully lifted the herringbone [as shown in Fig. 4(b)]; the resulting islands were larger than in the high-coverage systems. The largest islands were observed for the 0.62 ML system, which is entirely expected in light the proposed mechanism.

There was no step restructuring, or “faceting,” observed in the systems examined, which is expected given the proposed mechanism of surface reorganization. At full monolayer coverage, Au adatom diffusion distances were limited due to high molecular density. As such, Au adatoms did not migrate to the step edges and faceting did not occur. In all other systems studied the molecular density was low enough the adatoms migrated to nearby step edges. However, in each case the temperature was high enough that atoms along the steps could reorganize and did not appear faceted.

## B. Error analysis

The error margins associated with island measurements are relatively large and overlap in the case of measurements performed on the same initial coverage annealed to three different temperatures. The complexity and inhomogeneities present in these systems make them somewhat difficult to characterize. The broad distributions in island sizes (shown in the histograms provided in Fig. 6) and local island density are the main factors contributing to the difficulty in making precise measurements for percent island coverage. The added process of Au atom diffusion to nearby step edges and defects further complicates the system. Thus, the error bar reported does not reflect an error in the experimental measurement itself, rather the complex and inhomogeneous nature of the system as a whole.

## IV. CONCLUSIONS

Previously, we postulated that Au islands originated solely from the excess atoms in the herringbone reconstruction, as evidenced by the lack of etch pit formation. Indeed, our measurements of the Au islands revealed that island coverage never exceeded 4.4% across all molecular coverages examined. The interaction between TMP and the Au surface was strong enough that the molecules adsorbed and lifted the herringbone reconstruction but was not so strong as to eject additional atoms and create etch pits. This observation is in direct contrast with that observed when thiol molecules self-assemble on Au, which requires excess atoms to be removed from the surface and participate in adatom mediated bonding of the molecules.<sup>1,9</sup>

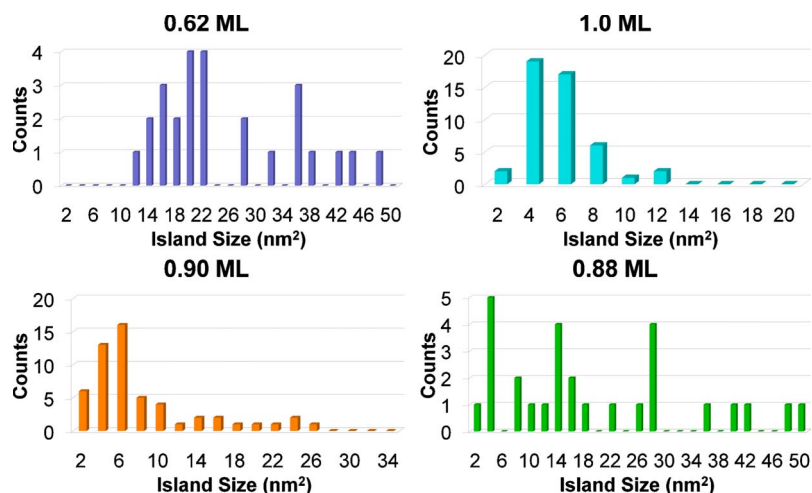


FIG. 6. (Color online) Histograms of Au adatom island sizes for each of the four trimethylphosphine-Au(111) system studied.

To summarize, we have shown that altering the headgroup element of a self-assembled monolayer can drastically affect Au surface restructuring upon adsorption. Upon TMP adsorption and subsequent annealing, the extra 4.4% Au atoms were forced out of the surface and the herringbone reconstruction disappeared as the surface atoms reorganized, ultimately adopting a  $(1 \times 1)$  configuration. Subtle changes in the surface binding strength of SAMs affected by either changing the anchoring group (as in this work) or by chemically altering the thiol head group through alkyl chain func-

tionality may offer new routes to more defect-free monolayers.

#### ACKNOWLEDGMENTS

We gratefully acknowledge support of this research by the National Science Foundation, the Department of Energy, Research Corporation, and the Beckman Foundation. A.D.J. acknowledges support from the National Science Foundation. H.L.T. acknowledges support from the Department of Education.

\*Corresponding author; charles.sykes@tufts.edu

- <sup>1</sup>P. Maksymovych, D. C. Sorescu, and J. T. Yates, *Phys. Rev. Lett.* **97**, 146103 (2006).
- <sup>2</sup>N. A. Kautz and S. A. Kandel, *J. Am. Chem. Soc.* **130**, 6908 (2008).
- <sup>3</sup>G. Nenchev, B. Diaconescu, F. Hagelberg, and K. Pohl, *Phys. Rev. B* **80**, 081401 (2009).
- <sup>4</sup>N. A. Kautz and S. A. Kandel, *J. Phys. Chem. C* **113**, 19286 (2009).
- <sup>5</sup>M. Yu, N. Bovet, C. J. Satterley, S. Bengio, K. R. J. Lovelock, P. K. Milligan, R. G. Jones, D. P. Woodruff, and V. Dhanak, *Phys. Rev. Lett.* **97**, 166102 (2006).
- <sup>6</sup>F. S. Li, W. C. Zhou, and Q. M. Guo, *Phys. Rev. B* **79**, 113412 (2009).
- <sup>7</sup>B. K. Min, A. R. Alemozafar, M. M. Biener, J. Biener, and C. M. Friend, *Top. Catal.* **36**, 77 (2005).
- <sup>8</sup>S. M. Driver, T. F. Zhang, and D. A. King, *Angew. Chem., Int. Ed.* **46**, 700 (2007).
- <sup>9</sup>P. Maksymovych and D. B. Dougherty, *Surf. Sci.* **602**, 2017 (2008).
- <sup>10</sup>H. Gronbeck, *J. Phys. Chem. C* **114**, 15973 (2010).
- <sup>11</sup>P. Maksymovych, D. C. Sorescu, and J. T. Yates, *J. Phys. Chem. B* **110**, 21161 (2006).
- <sup>12</sup>A. Nagoya and Y. Morikawa, *J. Phys.: Condens. Matter* **19**, 365245 (2007).
- <sup>13</sup>R. Mazzarello, A. Cossaro, A. Verdini, R. Rousseau, L. Casalis, M. F. Danisman, L. Floreano, S. Scandolo, A. Morgante, and G.

Scoles, *Phys. Rev. Lett.* **98**, 016102 (2007).

- <sup>14</sup>J. C. Love, L. A. Estroff, J. K. Kriebel, R. G. Nuzzo, and G. M. Whitesides, *Chem. Rev.* **105**, 1103 (2005).
- <sup>15</sup>T. A. Baker, E. Kaxiras, and C. M. Friend, *Top. Catal.* **53**, 365 (2010).
- <sup>16</sup>U. B. Steiner, P. Neuenschwander, W. R. Caseri, U. W. Suter, and F. Stucki, *Langmuir* **8**, 90 (1992).
- <sup>17</sup>H. Kariis, G. Westermark, I. Persson, and B. Liedberg, *Langmuir* **14**, 2736 (1998).
- <sup>18</sup>K. Uvdal, I. Persson, and B. Liedberg, *Langmuir* **11**, 1252 (1995).
- <sup>19</sup>G. Westermark, H. Kariis, I. Persson, and B. Liedberg, *Colloids Surf., A* **150**, 31 (1999).
- <sup>20</sup>G. Westermark and I. Persson, *Colloids Surf., A* **144**, 149 (1998).
- <sup>21</sup>D. J. Lavrich, S. M. Wetterer, S. L. Bernasek, and G. Scoles, *J. Phys. Chem. B* **102**, 3456 (1998).
- <sup>22</sup>J. L. Methot and W. R. Roush, *Adv. Synth. Catal.* **346**, 1035 (2004).
- <sup>23</sup>T. Trindade, P. O'Brien, and X. M. Zhang, *Chem. Mater.* **9**, 523 (1997).
- <sup>24</sup>D. E. Brown, D. J. Moffatt, and R. A. Wolkow, *Science* **279**, 542 (1998).
- <sup>25</sup>J. de la Figuera, K. Pohl, O. R. de la Fuente, A. K. Schmid, N. C. Bartelt, C. B. Carter, and R. Q. Hwang, *Phys. Rev. Lett.* **86**, 3819 (2001).
- <sup>26</sup>B. Voigtländer, G. Meyer, and N. M. Amer, *Phys. Rev. B* **44**,

- 10354 (1991).
- <sup>27</sup>J. A. Stroschio and D. M. Eigler, *Science* **254**, 1319 (1991).
- <sup>28</sup>D. D. Chambliss, R. J. Wilson, and S. Chiang, *J. Vac. Sci. Technol. B* **9**, 933 (1991).
- <sup>29</sup>J. A. Meyer, I. D. Baikie, E. Kopatzki, and R. J. Behm, *Surf. Sci.* **365**, L647 (1996).
- <sup>30</sup>M. M. Biener, J. Biener, and C. M. Friend, *Surf. Sci.* **601**, 1659 (2007).
- <sup>31</sup>F. Rossel, P. Brodard, F. Patthey, N. V. Richardson, and W. D. Schneider, *Surf. Sci.* **602**, L115 (2008).